An Optimization Framework for Inversely Estimating Myocardial Transmembrane Potentials and Localizing Ischemia

Dafang Wang, Robert M. Kirby, Rob S. MacLeod, and Chris R. Johnson

***Abstract*— By combining a static bidomain heart model with a torso conduction model, we studied the inverse electrocardiographic problem of computing the transmembrane potentials (TMPs) throughout the myocardium from a body-surface potential map, and then used the recovered potentials to localize myocardial ischemia. Our main contribution is solving the inverse problem within a constrained optimization framework, which is a generalization of previous methods for calculating transmembrane potentials. The framework offers ample flexibility for users to apply various physiologically-based constraints, and is well supported by mature algorithms and solvers developed by the optimization community. By avoiding the traditional inverse ECG approach of building the lead-field matrix, the framework greatly reduces computation cost and, by setting the associated forward problem as a constraint, the framework enables one to flexibly set individualized resolutions for each physical variable, a desirable feature for balancing model accuracy, ill-conditioning and computation tractability. Although the task of computing myocardial TMPs at an arbitrary time instance remains an open problem, we showed that it is possible to obtain TMPs with moderate accuracy during the ST segment by assuming all cardiac cells are at the plateau phase. Moreover, the calculated TMPs yielded a good estimate of ischemic regions, which was of more clinical interest than the voltage values themselves. We conducted finite element simulations of a phantom experiment over a 2D torso model with synthetic ischemic data. Preliminary results indicated that our approach is feasible and suitably accurate for the common case of transmural myocardial ischemia.**

***Index Terms*— Inverse Problem, Electrocardiography, Finite Element Method, Myocardial Ischemia, Constrained Optimization**

I. Introduction

A leading cause of death in the western world, myocardial ischemia (or more severely, infarction) occurs when cardiac myocytes are damaged for lack of oxygen or nutrients, normally caused by occlusion of coronary arteries. Electrocardiographic (ECG) diagnosis of myocardial ischemia relies on detecting the elevation/depression of the normally isoelectric ST segment, which is caused by the injury currents resulting from the transmembrane voltage difference between healthy and ischemic tissues. However, ECG-morphology analysis has limited ability to localize ischemic regions, and a computerized method achieving that function would effectively promote clinical diagnosis and treatment. We attempted to localize ischemia by inversely computing the transmembrane potentials (TMPs) throughout the myocardium from the voltages measured at the body surface. We proposed a constrained optimization framework for solving this inverse source problem, which is the main contribution of this paper.

The TMP is typically the source model for myocardial ischemia studies. While there are extensive studies on inverse ECG problems recovering epicardial potentials or activation sequences, research has been limited on reconstructing TMPs within the heart from the body-surface potentials. Because of its ill-posed nature, it still remains an open problem to accurately calculate myocardial TMPs at an arbitrary time instance. Methods for localizing myocardial ischemia have been proposed such as the model-based optimization, the level set method, or calculating the ST-segment integral of TMPs [1], but they do not directly calculate TMPs.

Our study was based on the hypothesis that one may obtain modestly accurate TMPs at one time instant in the ST interval. Although the reconstructed voltage values are not sufficiently accurate for precise quantification of the TMPs, their qualitative "patterns" may enable a satisfying recovery of the size and position of ischemic regions. We modeled the ECG problem by combining a mono-domain torso model with a static bidomain heart model, which represents the cardiac source by the distribution of TMPs. A framework for computing TMPs was proposed in [2], in which the inverse problem was formulated as a minimization problem constrained by the associated forward problem, and was solved by a one-shot adjoint method. This framework is limited to quadratic objective functions with equality constraints only. We generalized their constrained optimization framework so as to enable broader types of objective functions, both equality and inequality constraints, and flexibility for applying various physiologically-based constraints. It also has two advantages over the traditional way of solving inverse ECG problems, which first forms a lead-field matrix and then "inverts" it by regularization techniques. First, our method does not compute the lead-field matrix and thus has lower computational cost. Second, it allows a flexible setting of the discretization resolution for the TMPs and other state variables, a desirable feature as the ill-posed inverse problem typically requires different resolutions for the sought-for unknowns and other state variables [3], [4].

II. Methods

1) The Bioelectric Model: Our bioelectric model consists of a static bidomain heart model combined with a mono-domain torso model, as shown in Fig 1(B). The combined model can be simply written as a Poisson equation as

Wang, Kirby, MacLeod and Johnson are with the Scientific Computing and Imaging Institute, University of Utah. Email: {dfwang, kirby, macleod, crj}@sci.utah.edu

This work was funded in part by NSF Career Award NSF-CCF0347791 and NIH NCRR Center for Integrative Biomedical Computing Grant No. 5P41RR012553-12.

follows:

$$\nabla \cdot \sigma \nabla u(\boldsymbol{x}) = \begin{cases} 0, & \boldsymbol{x} \in \Omega, \\ -\nabla \cdot \sigma_i \nabla v(\boldsymbol{x}), & x \in H, \end{cases} \quad (1)$$

$$\vec{n_T} \cdot \sigma \nabla u(\boldsymbol{x}) = 0, \quad \boldsymbol{x} \in \partial\Omega, \quad (2)$$

$$u(\boldsymbol{x}) = \begin{cases} \text{torso potential}, & x \in \Omega, \\ \text{extracellular potential}, & x \in H, \end{cases} \quad (3)$$

$$\sigma(\boldsymbol{x}) = \begin{cases} \sigma_i + \sigma_e, & x \in H, \\ \sigma_t, & x \in \Omega. \end{cases} \quad (4)$$

The first row of (1) describes the passive torso volume conductor Ω, and the second row describes the static bidomain equation for the heart H. We only considered the static bidomain because the TMP (denoted by v) remains largely stable during the plateau phase. σ_i and σ_e are the intra/extracellular conductivity, and σ_t is the conductivity of torso tissues. Eq (2) implies no electrical currents leave the torso surface, Γ_T. This model implicitly assumes three boundary conditions at the heart/torso interface: 1) the extracellular potential is continuous; 2) the electrical current flowing out of the heart is equal to that flowing into the torso; and 3) the cardiac intracellular space is insulated from the torso. Details of the model can be found in Chapter 5 of [5].

In this study, we solved (1) by the finite element method, which converts the Poisson equation into a matrix system:

$$\boldsymbol{A}u = \mathbf{S}v \quad (5)$$

where A and S are the stiffness matrix corresponding to the operator on each side of (1). Given v, the task of solving (5) for u is referred to as the associated forward problem.

2) The Ischemia Model: We adopted a synthetic ischemia model represented by the TMP at the plateau phase, given as follows:

$$v(x) = \begin{cases} 0\ mV, & \text{in healthy tissue;} \\ -30\ mV, & \text{in ischemic tissue;} \end{cases} \quad (6)$$

where the assumed 30mV voltage difference is an approximation suggested by previous studies [6]. The value is not critical to the simulations because of the threshold operation performed on the solution (see sections below). Although very simplified, the binary assumption of the TMP is not critical to the inverse simulation because our inverse calculation incorporated no *a priori* information of the TMP field. When implementing (6) by the finite element method, we assumed a linear transition of $v(x)$ at the border zone, which comprises the first layer of elements surrounding the ischemic region. With this model, we simulated the effect of myocardial ischemia of different locations and sizes.

3) Traditional Methods for Inverse Problems: The traditional way of solving our inverse ECG problem is to derive from (5) a lead-field matrix $\mathbf{K}$ that relates v and the torso-surface potential u_T: $u_T = \mathbf{K}v$. Because $\mathbf{K}$ is ill-conditioned, regularization such as the Tikhonov method is applied to obtain v:

$$v = argmin \ \{\|\mathbf{K}v - u_T\|_2 + \lambda\|\mathbf{W}v\|_2\}, \quad (7)$$

where $\mathbf{W}$ describes the property of v to be constrained. Although this approach is popular among other inverse ECG problems (e.g., recovering epicardial potentials), its computational cost becomes prohibitive when applied to the inverse problem considered in this paper. Suppose the discrete Poisson equation (5) has a size of m and v has a size of n, deriving the lead-field matrix requires one to solve a m by m linear system for n times. For a bidomain model in three dimension, m and n can easily reach hundreds of thousands.

Nielson *et al*[2] avoided the lead-field matrix by forming the inverse problem as a constrained optimization problem:

$$v = \underset{v}{argmin} \left\{\|\mathbf{Q}u - u_T\|_2^2 + \lambda\|\mathbf{W}v\|_2^2\right\}, \quad (8)$$

$$\text{subject to} \quad \boldsymbol{A}u = \mathbf{S}v, \quad (9)$$

where $\mathbf{Q}$ maps the potential field u to the measurement location. This formulation is equivalent to the Tikhonov method (7) except that u and v are related by a constraint equation. The minimization was repeated with a decreasing sequence of λ until the misfit $\mathbf{Q}u - u_T$ reached the noise level, which was known. For each λ, the constrained minimization was achieved by analytically solving its KKT conditions, which happened to be a system of linear equations. This method, however, is limited to quadratic objective functions and equality constraints, for otherwise the KKT equations would be non-linear. Another drawback is that the minimization starts from scratch with each λ. Given that normally 100 λs are to be tested, the minimization process may become slow and inefficient.

4) Constrained Optimization Framework: We generalized the above optimization framework, allowing both equality and inequality constraints and l_p-norms in the objective function. The framework is presented below:

$$v = \underset{v}{argmin}\|\mathbf{W}(v - v_{prior})\|_p, \quad (10)$$

$$\text{subject to} \quad \boldsymbol{A}u = \mathbf{S}v, \quad (11)$$

$$\text{and} \quad \|\mathbf{Q}u - u_T\|_2 \leq \epsilon\|u_T\|_2, \quad (12)$$

$$\text{and} \quad v \leq 0, \quad (13)$$

where all terms have been defined before. Equation (12) states that the misfit between the predicted data and the measured data (u_T) should be within the noise level ϵ, which is known. Equation (11) and (12) are the "necessary" constraints, whereas (13), which assumes that TMPs should be no greater than 0mV, exemplifies how one may flexibly add physiologically-based constraints into the framework. The framework also offers flexibility for one to choose an objective function other than the l_2 norm, *e.g.*, l_1-norm minimization is often preferable.

Our proposed constrained optimization has been well-studied by the optimization community. The simplest case is l_2-norm minimization with equality constraints, where one may solve the KKT conditions analytically. The second level is equality constraints with a convex objective function, where the optimization problem can be reduced to an unconstrained optimization problem and then solved by Newton's method. Inequality constraints form the next level in the hierarchy, where the problem can be transformed into

a second-order cone program and solved by interior point methods (*e.g.*, log-barrier algorithm), with the philosophy of reducing an inequality-constrained problem to a sequence of equality-constrained problems. Mature methodologies and solvers are available in this field [7]. We used CVX, a package for specifying and solving convex programs [8].

It is worth mentioning that our framework is equivalent to the previous methods (7) or (8), but without needing to tune the parameter λ. Instead the tuning is fulfilled when executing interior-point methods and is often more efficient. For example, when the log-barrier method minimizes a sequence of sub-problems, the solution of the previous sub-problem becomes the initial guess of the next one. In contrast, when λ is tuned in (7) and (8), calculation starts from scratch.

5) Simulation Setup: We conducted finite element simulation based on a 2D thorax domain illustrated in Fig 1. All potential fields were defined on mesh nodes. As the goal of this study was to validate the feasibility of the optimization method, we minimized the effect of the conductivities by using simple phantom values. The conductivities are given as $\sigma_i = \sigma_e = [0.5, 0.5]$ and $\sigma_t = [1.0, 1.0]$, along the longitudinal and transverse directions, respectively.

In each simulation, we first specified an ischemic region and set the synthetic TMP values according to (6). We then performed forward simulation to obtain the torso-surface potentials, which, after being contaminated with noise, served as the input for the inverse calculation. Ischemic regions were estimated from the calculated TMP field by the following criterion: if the TMP at a node was below a threshold value, the node was an ischemic site and all elements adjacent to this node were regarded as ischemic regions. The threshold value for a given TMP field v was determined by

$$threshold = mean(v) - 0.4(mean(v) - min(v)), \quad (14)$$

based on the hypothesis that the TMP at an ischemic site should be notably below the average TMP voltage because ischemic regions were assumed to account for a minor part of the myocardium.

6) Evaluating the Shape of Ischemia: Besides visual comparison, we quantitatively evaluated how close the reconstructed ischemic region is to the "true" region by two metrics: the centroid distance, which measures the distance between the centers of two shapes, and the Hausdorff distance, which is defined below for two shapes X and Y:

$$\text{Hdist} = max\ \{\max_{x\in X}\ \min_{y\in Y}\ d(x,y),\ \max_{y\in Y}\ \min_{x\in X} d(x,y)\ \}$$

where $d(x, y)$ denotes the Euclidean distance between points x and y. The Hausdorff distance means that, from any point in either shape, one is guaranteed to reach a point in the other shape within the Hausdorff distance. The Hausdorff distance measures the proximity of "contour" of two shapes, whereas the centroid distance measures the proximity of "position".

III. Results

1) Ischemia Setup: Fig 1 shows a case of left anterior transmural ischemia and its resulting extracellular potential field (the forward solution). In following sections, reconstructed values are to be compared with this "ground truth". Recall that the TMPs were -30mV for ischemic region and 0mV for health region.

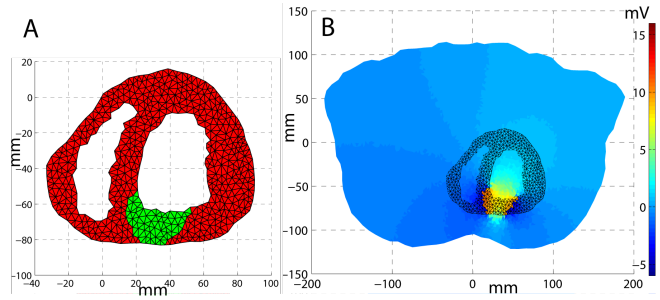

Fig. 1. (A): the "true" ischemic region denoted by the green color. (B): the resulting extracellular potential field. The mesh contains 9610, 1005 and 498 triangle elements in the torso volume, the myocardium and the ventricular cavities, respectively. Only the myocardium mesh is shown.

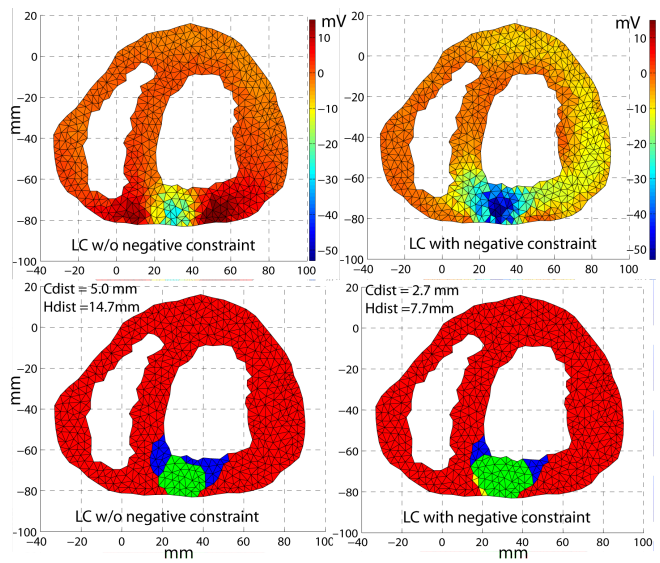

Fig. 2. Inverse solutions obtained by applying a Laplacian constraint (LC) on the TMPs, with and without the extra negative constraint (13). The input body-surface potentials were corrupted with 30dB white noise. The top row shows the calculated TMPs. The bottom row compares the true ischemic region with the one inferred by thresholding. Red color: healthy tissue. Green: the ischemic tissue that was correctly recovered. Blue: the ischemic tissue that was not recovered. Yellow: healthy tissue but incorrectly judged to be ischemic. The centroid distance (Cdist) and Hausdorff distance (Hdist) are given for each detected ischemic region.

2) Solution by Inequality Constraints: Here we present an example of calculating the TMP using the general optimization framework (10)-(12). We constrained the Laplacian of the TMPs by letting $\mathbf{W}$ be a discrete Laplacian operator obtained by second-order Taylor expansion at each node. From recovered TMPs, ischemic regions were identified by the thresholding (14). The results are shown in Fig 2. Since the optimization here was equivalent to the second-order Tikhonov regularization, the calculated TMPs were smoothed compared to the true values. However, with proper color rescaling one may see that the recovered TMPs preserved the polarity of the original field, thereby enabling a satisfactory

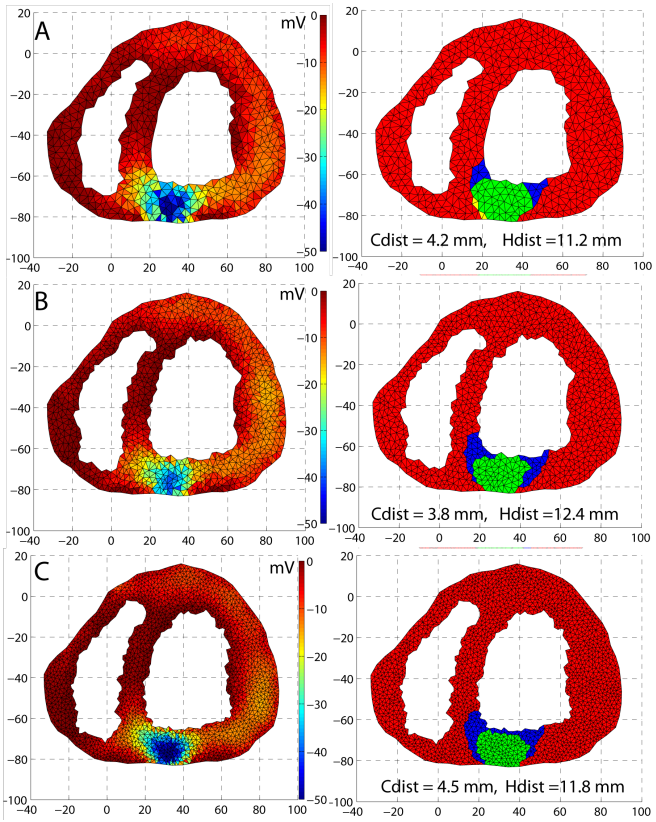

Fig. 3. Inverse simulations with three heart models. Each row shows the calculated TMPs (left) and the inferred ischemic regions (right). The second-order constraint along with the negative constraint was used, and 30dB input noise was added on the body-surface potential. Heart A has 600 nodes and 1005 triangle elements. Heart B has 890 nodes and 1530 elements. Heart C has 1716 nodes and 3093 elements. The color code for the right column is given as follows. Red: healthy tissue. Green: the ischemic tissue that was correctly recovered. Blue: the ischemic tissue that was not recovered. Yellow: healthy tissue but incorrectly judged to be ischemic. The centroid distance (Cdist) and Hausdorff distance (Hdist) are given for each detected ischemic region.

estimate of the ischemic region after a simple thresholding.

Fig 2 also shows how the inverse solution was notably improved by adding even a simple negative constraint (13). The regular Laplacian constraint yielded spurious elevations of TMP in the regions near the ischemic zone where the TMP there was expected to be the same as the rest of the heart. Adding the negative constraint not only removed this artifact, but also enhanced the TMP difference between the ischemic and healthy regions, and thereby yielded better ischemia recovery by both visual and quantitative assessments (see the centroid and Hausdorff distances). In real situations, the upper bound of TMPs may not be 0mV. A good substitute estimate would be the average of a fast-obtained inverse solution.

3) Multi-Resolution Study: The multi-resolution study has two goals: 1) to examine the robustness and scalability of our optimization framework, and 2) to explore how resolution will impact the numerical ill-conditioning of the inverse problem. This study helps researchers to discretize the bioelectric model with proper fidelity so as to achieve a good balance between model accuracy and numerical difficulty. We conducted a preliminary multi-resolution study by testing the optimization framework on three heart models, as shown in Fig 3. When increasing the model fidelities, the inverse solutions remained largely consistent but were not significantly improved, indicating that a well-refined model may not be cost-effective for inverse simulations.

IV. Discussion and Conclusion

This paper reports our initial investigation of estimating myocardial ischemia by inversely computing the myocardial TMPs from body-surface potentials. Our main contribution was a constrained optimization framework for solving the inverse ECG problem. The framework was a generalization of previous methods and provided ample flexibility for users to apply various physiologically-based constraints so as to improve the inverse solutions. By avoiding deriving the lead-field matrix as in traditional approaches, the framework greatly reduced computation. Moreover, because the framework incorporated as a constraint the associated forward problem, which dictates the relationship of all physical variables, it enabled one to flexibly adjust individualized resolutions for each physical variable during the inverse calculation. Such adjustment is often necessary when solving inverse problems, in order to balance the model accuracy, ill-conditioning, and computation cost. In contrast, in tradition methods each resolution adjustment requires the lead-field matrix be completely recalculated. Finally, the framework was also well supported by mature, reliable algorithms and packages.

Our future work includes extending this framework to simulations in 3D and exploring advanced constraints. With realistic anatomical models in 3D, the problem size and computation cost will become a major concern, so an important study would be to identify the model resolution that balances accuracy, ill-conditioning and computation cost.

References

[1] Y. Jiang, C. Qian, R. Hanna, D. Farina, and O. Dössel, "Optimization of the electrode positions of multichannel ecg for the reconstruction of ischemic areas by solving the inverse electrocardiographic problem," *Int. Jrnl of Bioelectromagnetism*, vol. 11, no. 1, pp. 27–37, 2009.

[2] B. F. Nielsen, X. Cai, and M. Lysaker, "On the possibility for computing the transmembrane potential in the heart with a one shot method: An inverse problem," *Math. Biosci.*, vol. 210, no. 2, pp. 523–553, 2007.

[3] D. Wang, R. M. Kirby, and C. R. Johnson, "Resolution strategies for the finite-element-based solution of the ecg inverse problem," *IEEE Trans Biomed Eng*, vol. 57, no. 2, pp. 220–237, 2010.

[4] ——, "Finite-element-based discreitzation and regularization strategies for 3d inverse electrocardiography," *IEEE Trans on Biomed Eng, accepted*, 2011.

[5] R. M. Gulrajani, *Bioelectricity and biomagnetism*. John Wiley & Sons Inc, 1998.

[6] D. Li, C. Y. Li, A. C. Yong, and D. Kilpatrick, "Source of electrocardiographic st changes in subendocardial ischemia," *Circ. Res.*, vol. 82, pp. 957–970, 1998.

[7] S. Boyd and L. Vandenberghe, *Convex Optimization*. Cambridge University Press, 2004.

[8] M. Grant and S. Boyd, "CVX: Matlab software for disciplined convex programming, version 1.21," 2011.